# On the Low-Frequency Motions in the Cilician Basin

ÜMIT ÜNLÜATA

*Department of Marine Science, Middle East Technical University, P.K. 28, Erdemli, Icel, Turkey*

(Manuscript received 25 April 1980, in final form 26 October 1980)

ABSTRACT

The presence of low-frequency motions in the Cilician Basin (the northeastern Mediterranean Sea) is investigated. An $f$-plane, barotropic, wind-driven model is utilized by taking advantage of the channel-like geometry of the basin. An asymptotic method (Allen, 1976) is employed to decouple the channel proper from its narrow and steep coastal margins. A resonant response is predicted at the cut-off frequencies for which the group velocities vanish. Both this resonant response and another form of resonance are discussed. Partial support is found from available data.

## 1. Introduction

The region of the northeastern Mediterranean lying between Turkey and the northern coast of Cyprus is known (in geological terms) as the Cilician Basin (Fig. 1). The distinguishing feature of the eastern Mediterranean, in general, and of the Cilician Basin in particular, is that very little is known about the dynamics of these waters. A mean cyclonic circulation in the eastern Mediterranean evidently exists (Lacombe and Tchernia, 1972). Some ship observations have been statistically analysed and compiled by the Royal Netherlands Meteorological Institute (RNMI) (1957), but aside from these, the available information is patchy and quite meager.

A cursory examination of winds over the eastern Mediterranean at large reveals northerlies and northwesterlies (RNMI, 1957). On the other hand, a striking variability of winds, both in space and time, can be observed in the Cilician Basin and this is reflected in currents as well as other oceanographic parameters. High intensity and reversible currents distinguish the region from the rest of the eastern Mediterranean (see also Hydrographer of the Navy, 1976).

The variability of the local winds is attributable to many factors. The region lies along the tracks of wintertime cyclones (Palmén and Newton, 1969). Due to the presence of the Taurus mountain chain along the entire southern Turkish coast, local cyclogenesis does take place in a fashion that is similar to that known as Alpine cyclogenesis (Tibaldi, 1979). In addition, a mesoscale opening in the mountain chain directly across the Cyprus leads to strong northeasterlies (80–125 km $h^{-1}$) that form a wind belt over the central Cilician Basin. This wind system is similar to the Mistral of southern France (Bunker and Cornell, 1971) and it is also present during summer as a thermally-driven system. In summer a strong seabreeze (6–15 m $s^{-1}$) is also present. The details of the meteorological aspects of the region are beyond the scope of this paper. Here we fix our attention on the low-frequency variability of the currents.

Experimental data collected during 1977–80 at two locations along the southern Turkish coast have revealed the existence of relatively intense, low-frequency currents (due to gaps present in most of the data, only two long-term observations are considered here).

The nature of the observed low-frequency motions are investigated via an $f$-plane analytical model of barotropic motions over topography (Allen, 1976). The section of the Cilician Basin lying between the northern coast of Cyprus and Turkey is modeled as a channel with topography having shelf regions along its east–west running boundaries.

The model proposed here is similar to that of Brooks and Mooers (1977) for the Florida straits. A mean current with the intensity of the Florida current is absent in the present situation. However, advantage is taken of the following fact to build an analytical model: The shelf along the Turkish coast is very narrow and rapidly joins the main part of the channel (*the interior*) and furthermore it is difficult to imagine a shelf area along the Cypriot coast. This fact allows the employment of an asymptotic method due to Allen (1976). It is found that, to a first order of approximation, the interior motions are decoupled from the shelf areas and provide partial forcing to them.

An analysis of free motions (Section 3) reveals the

0022-3670/82/020134-10$06.50

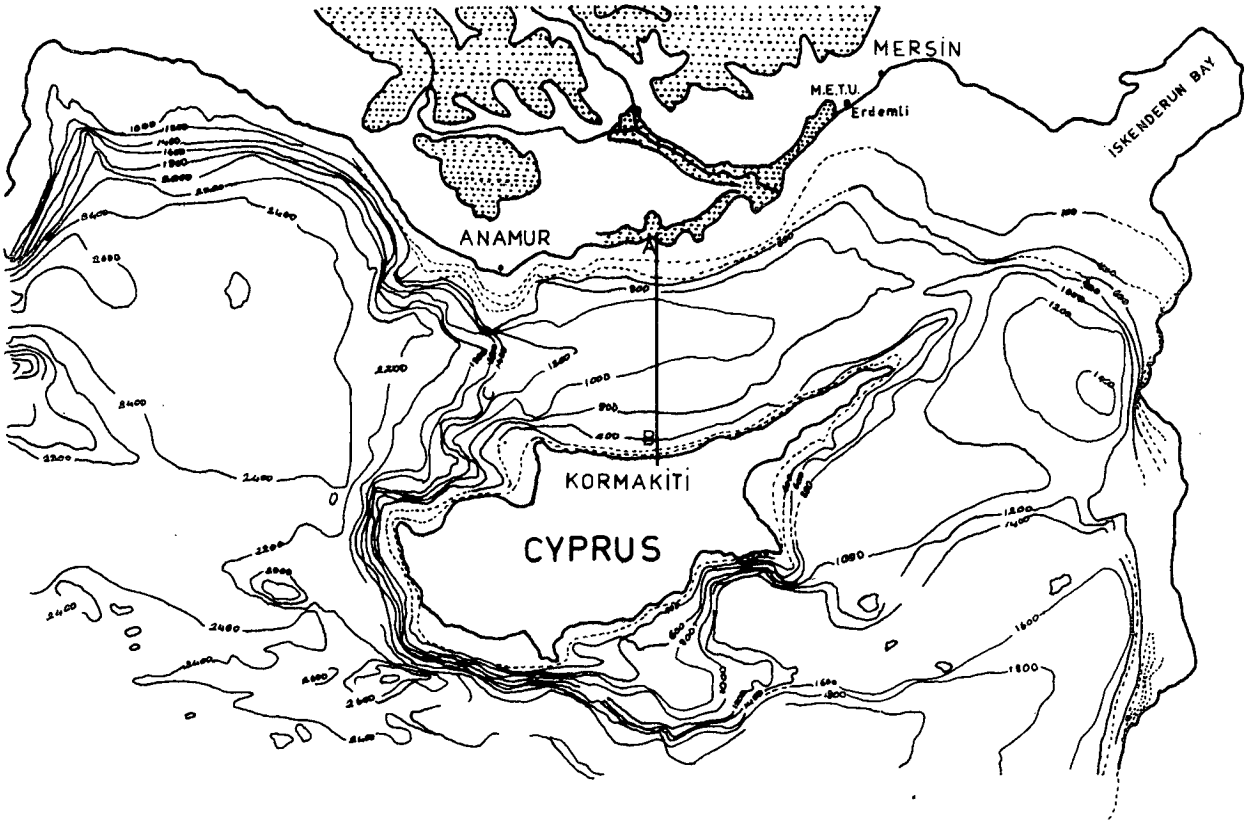


FIG. 1. The bathymetry of the Cilician Basin which is defined here as the region between the northern coast of Cyprus and the southern coast of Turkey. Submarine contours in meters.

existence of a set of evanescent modes that accompany the expected topographic Rossby-wave modes of a channel (Pedlosky, 1979). It is found that through the forcing of the interior, a resonant response of one of the shelf areas is possible. This occurs when the phase speed of one of the topographic Rossby modes of the interior coincides with the phase speed of a free continental-shelf wave mode, the latter speed being determined by isolating the shelf area from the interior (Gill and Schumann, 1974).

For the Cilician Basin the aforementioned resonant tuning is not possible. However, the interior (and subsequently the shelf) can resonate whenever the frequency of the wind-forcing coincides with one of the cutoff frequencies at which the modal group velocities vanish. This is demonstrated in Section 4 by considering forced motions in an infinite channel, a semi-infinite channel and a closed basin. The closure of the channel at one end is an approximation to the end conditions of the Cilician Basin in the east. The analysis of the closed basin oscillations is a matter of curiosity. The precise modeling of the wind-stress distribution in space is not important in that the main focus is on the resonant tuning through frequency.

We do not claim that the geometry of the present results reflects the real complexities of the Cilician Basin. In essence, we have focused on the wave trapping by the east–west running boundaries and partial support for this possibility is found from observations (Section 5).

## 2. Formulation of the problem

We consider wind-induced, barotropic motions occurring on an $f$-plane and within semi-enclosed and enclosed basins with topography. The geometries of interest consist of an infinite channel, a semi-infinite channel and a rectangular basin (Fig. 2). A Cartesian coordinate system is adopted such that the $x$ axis points towards north and the $y$ axis is aligned with the coastline on the southern boundary of each system, pointing towards west.

We let $L$ denote the width (along $x$) and $H_0$ the scale depth of the systems under consideration. For the Cilician Basin, $L \simeq 100$ km and $H_0 \simeq 1$ km. The latitude of the basin is $\simeq 36°$N and therefore $(fL)^2/gH_0 \ll 1$, where $f$ is the Coriolis parameter and $g$ the gravitational constant. The smallness of the above parameter allows a non-divergent approximation for the continuity equation (Adams and Buchwald, 1969). The inviscid, linearized and vertically aver-

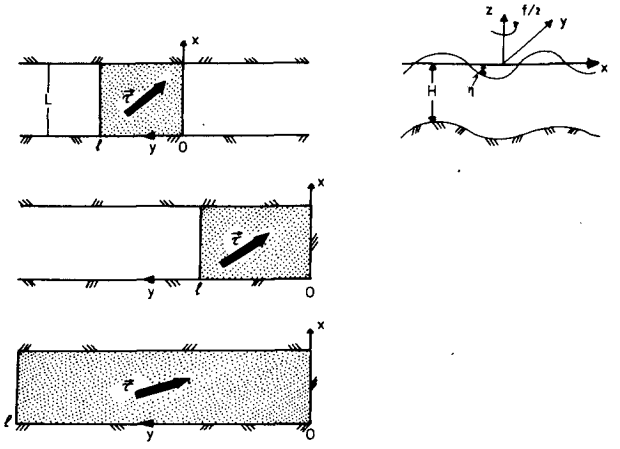

FIG. 2. Definition sketches of models considered.

aged equations of motion are consequently of the form

$$\mathbf{u}_t + f\mathbf{k} \times \mathbf{u} = -g\nabla\eta + \tau/\rho H, \tag{2.1}$$

$$\nabla \cdot \mathbf{u}H = 0, \tag{2.2}$$

where the bottom friction has also been neglected. In Eqs. (2.1) and (2.2) $\mathbf{u}$ is the depth-averaged velocity with components $(u, v)$ along $(x, y)$, $\mathbf{k}$ is the unit vector along the vertical, $\eta$ the free surface displacement, $\tau = (\tau^x, \tau^y)$ the wind-stress, $\rho$ the density, $H$ the variable water depth, $t$ the time, and $\nabla$ the horizontal gradient operator and subscripts imply partial differentiation. The non-divergent approximation involves the neglecting of a $\eta_t$ term in (2.2) and, as a result, gravity waves are filtered out.

The variables $[\mathbf{u}, (x, y), t, \eta, \tau, H]$ are next scaled by $(U_0, L, f^{-1}, U_0fL/g, \rho U_0 f H_0, H_0)$ and Eq. (2.2) is utilized to introduce a stream function such that

$$H\mathbf{u} = -\mathbf{k} \times \nabla\Psi. \tag{2.3}$$

If depth variations are restricted to occur only in the transverse direction $(x)$, the following dimensionless vorticity equation then follows (Adams and Buchwald, 1969; Allen, 1976):

$$[\Psi_{xx} + \Psi_{yy} - (H_x/H)\Psi_x]_t + (H_x/H)\Psi_y = \tau_y{}^x - \tau_x{}^y + (H_x/H)\tau^y. \tag{2.4}$$

For a given depth variation, the primary task is to solve (2.4) subject to appropriate initial and boundary conditions.

### *a. An asymptotic method*

Even for a time-dependence of the form $e^{i\omega t}$, the finding of the solutions of (2.4) for arbitrary depth variations requires numerical techniques (Brooks and Mooers, 1977). Here we seek analytical solutions by considering basins with relatively wide and flat cross-sections that are flanked by narrow and steep continental shelves along the east-west-aligned coasts (Fig. 3). The situation envisioned is appropriate for the central Cilician Basin. The shelf area along the Turkish coast is at most 15–20 km in width, rapidly joining the deeper waters, while along the northern Cypriot coast there exists no significant shelf area (Fig. 4). Under such a condition, an asymptotic method due to Allen (1976) can be utilized to obtain analytical solutions. A very systematic exposé of the method is given by Allen and we therefore summarize here only the salient aspects.

If the length scale $L$ of the channel areas proper, called the *interior*, is much greater than the width of the relatively narrow and steep regions, then the motion in the interior is not affected by those occurring on the shelves. Consequently, the interior motions are decoupled from those on the shelf so that the appropriate boundary conditions for the leading-order interior motions are

$$\psi_y = 0, \quad x = 0, 1, \tag{2.5}$$

the governing equation being (2.4). On the other hand, the shelf motions are influenced by the interior through the pressure and flux continuity at the interior–shelf fluid boundaries. Consider first the shelf region along $x = 0$ which joins the interior at $x = \delta_1$ (Fig. 2). If the depth variation for $x \leqslant \delta_1$ is of the form

$$H = \exp[(x - \delta_1)/\delta_B\delta_1], \quad \delta_1 \ll 1, \quad \delta_B = O(1), \tag{2.6}$$

and if $t = O(\delta_1{}^{-1})$, then the streamfunction $\Psi^{(1)}$ for the leading-order shelf motion satisfies (Allen, 1976, Eqs. 2.21, 2.23, 2.25b)

$$\delta_1{}^{-1}(\delta_B\Psi_{\xi\xi}{}^{(1)} - \Psi_\xi{}^{(1)})_t + \Psi_y{}^{(1)} = \tau^y(x = 0, y, t), \tag{2.7a}$$

$$\Psi_y{}^{(1)} = 0, \quad \xi = 0, \tag{2.7b}$$

$$\Psi_{\xi t}{}^{(1)} = \tilde{\Psi}_{xt}{}^{(1)}, \quad \xi = 1, \quad x = 0, \tag{2.7c}$$

where $\xi = x/\delta_1$ is the stretched off–onshore coordinate, and $\tilde{\Psi}^{(1)} = \delta_1\Psi$ is the streamfunction of the

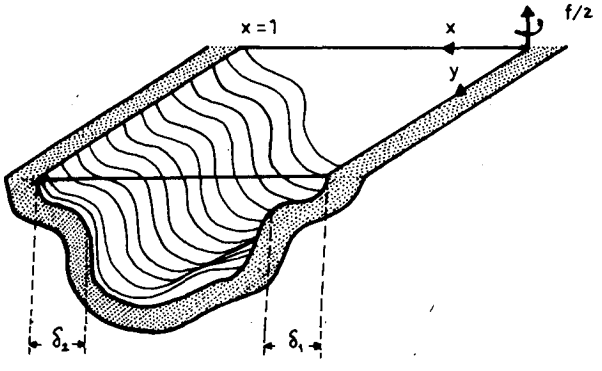

FIG. 3. The model bathymetry.

interior. Accordingly, the first task is to solve (2.4) for the interior motions by involving (2.5). The interior solution is then utilized in (2.7c) to solve for the motions on the shelf.

Similar analysis prevails for the shelf area along $x = 1$ with the assumed depth variation of the form

$$H = (H)_{x=1} \exp(1 - x - \delta_2)/\delta_B\delta_2, \quad 1 - \delta_2 < x < 1, \tag{2.8}$$

leading to

$$\delta_2^{-1}(\delta_B\Psi_{\mu\mu}^{(2)} - \Psi_\mu^{(2)})_t - \Psi_y^{(2)} = -\tau^y(x = 1, y, t), \tag{2.9a}$$

$$\Psi_y^{(2)} = 0, \quad \mu = 0, \tag{2.9b}$$

$$\Psi_{\mu t}^{(2)} = -\tilde{\Psi}_{xt}^{(2)}, \quad \mu = 1, \quad x = 1, \tag{2.9c}$$

where $\mu = (1 - x)\delta_2$, $\Psi^{(2)}$ refers to the shelf area and $\tilde{\Psi}^{(2)} = \delta_2\Psi$. The difference in the signs of some terms of (2.7) and (2.9) is due to the differences in depth variation across each shelf.

It is worth pointing out that the assumed timescale of the motions is of $O(\delta_1^{-1}) = O(\delta_2^{-1})$, i.e., much greater than the inertial period. The motions on the shelf regions are non-dispersive while those in the interior are not. Allen (1976) took the interior to be of constant depth. Here we will consider it to be slowly varying $[H_x/H = O(\delta)]$, but this is a simple extension of Allen's analysis.

According to the above formulation, the interior takes on the role of the driving oscillator, and the shelf regions the driven oscillators. The characteristics of the interior motions are thus of primary interest. A model for the depth variations in the channel is considered next.

### b. *Model equations for the interior*

As remarked earlier, the depth variation in the interior is assumed to be small. In order to simplify the problem, we assume for sufficiently small values of $b$,

$$H = e^{2bx}, \quad 0 \leqslant x \leqslant 1. \tag{2.10}$$

For the Cilician Basin proper, the estimated value of the constant $b \approx 0.17$. This corresponds to depths of 1000 m on the Turkish side and 700 m on the Cyprus side of the Basin.

Assuming a time-dependence of the form

$$\Psi = \psi e^{i\omega t}, \quad \tau = (T^x, T^y)e^{i\omega t}, \quad \mathbf{u} = (U, V)e^{i\omega t}, \tag{2.11}$$

and utilizing (2.10), the governing equation (2.4) for the interior problem reduces to

$$\nabla^2\psi - 2b(\psi_x + i\psi_y/\omega) = Q, \tag{2.12}$$

where

$$Q = (T_y^x - T_x^y + 2bT^y)/i\omega. \tag{2.13}$$

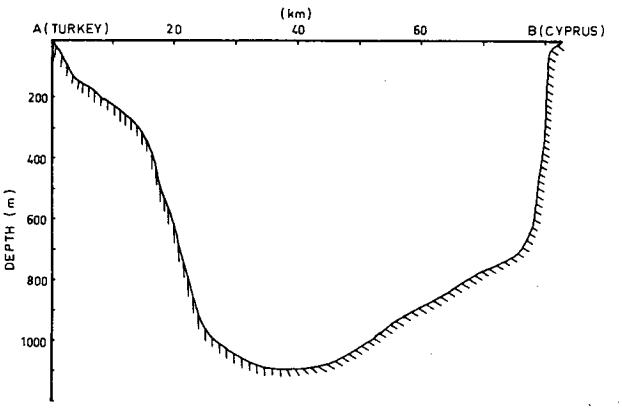


FIG. 4. Cross section of the Cilician Basin (see Fig. 1).

The appropriate boundary conditions at $x = 0, 1$, are given in (2.5) with $\psi$ replacing $\Psi$.

## 3. Free motions—infinitely long channel

### a. *Interior*

An examination of the possible modes of motion in an infinitely long channel in the absence of wind provides guidance to the analysis of the forced motions. With $Q$ set equal to zero the problem is essentially a waveguide-propagation problem and the general solution of (2.12) subjected to (2.5) is

$$\psi = \sum_{n=1}^{\infty} \psi_n(x)[\alpha_n^- \exp(ik_n^- y) + \alpha_n^+ \exp(ik_n^+ y)], \tag{3.1}$$

where

$$\psi_n = \exp(bx) \sin n\pi x, \tag{3.2}$$

$$k_n^\pm = (b/\omega)\{1 \pm [1 - (\omega/\omega_n)^2]^{1/2}\}, \tag{3.3}$$

$$\omega_n = b/[b^2 + (n\pi)^2]^{1/2}, \tag{3.4}$$

and where $\alpha_n^\pm$ are arbitrary constants.

Fixing $b$ and $\omega(>0)$, we infer from the solution above that for $\omega > \omega_1$, $k_n^\pm$ are complex for all $n$ and the motion can only decay with distance, the growing solutions being inadmissible. In other words all the modes of motion vanish for $\omega > \omega_1$. For $\omega_{m+1} < \omega < \omega_m$, $k_n^\pm$ are real for $n \leqslant m$ and $2m$ modes propagate, the remaining modes being evanescent.

The importance of the evanescent modes will become clear in later analysis. They imply wave motions whose amplitudes decay within a distance $(\omega/b)\{(\omega/\omega_n)^2 - 1\}^{-1/2}$. The vanishing modes are an undiscardable part of any motion in which an inhomogeneity is introduced.

The modes that propagate are the topographic Rossby waves. Even though their properties are well known (Pedlosky, 1979), a brief discussion of their salient properties is warranted here for the sake of

completeness and for providing assurance that the proper radiation conditions are invoked in the forced motions.

The propagative modes consist of a short- and a long-wave with wavenumbers $k_n^+$ and $k_n^-$, respectively. Both waves propagate in the $(-y)$ direction by taking the shallower water to their right. This is the usual property of the topographic waves (LeBlond and Mysak, 1978). The progressive modes imply dispersive waves with group velocities

$$C_{gn}^{\pm} = -\frac{d\omega}{dk_n^{\pm}} = \omega^2[k_n^{\pm} - (b/\omega)]/k_n^{\pm}b, \quad (3.5)$$

where the minus sign is introduced since the wave motion is like $\exp i(ky + \omega t)$ such that $\omega > 0$ and $k > 0$. A separate but lengthy analysis involving the computation of the cross-sectional average energy flux ensures that the group velocity as given in (3.5) has the proper signs. Utilizing Eq. (3.3), it is inferred from (3.5) that the shorter of the waves ($k_n^+$) radiates energy in the $(+y)$ direction, i.e., in the direction opposite to that of the phase propagation. On the other hand, the long wave modes with wave numbers $k_n^-$ radiate energy in the phase propagation direction. These radiation properties are important in invoking the proper radiation conditions in the forced motions. It is worth pointing out that similar results apply to planetary Rossby waves on a $\beta$-plane (Fofonoff, 1962). This is as expected in view of the known similarities between topographic and planetary waves (Pedlosky, 1979).

An important property of the group velocity is that it vanishes for $\omega = \omega_n$. This result is similar to that found for the continental shelf waves (Buchwald and Adams, 1968). The dimensionless frequencies $\omega_n$ are the cut-off frequencies also encountered in other types of wave-guides (Collin, 1960). In the forced motions a resonant response is expected whenever the impressed frequency becomes equal to $\omega_n$, for then the energy radiation should diminish.

The cutoff frequencies form a dense set in that for small $b$ (or large $n$), $\omega_n \approx b/n\pi$ so that $\omega_n - \omega_{n+1} \approx 1/n^2$, implying closely-ordered spectral lines. It is interesting to note that the cutoff frequencies are ordered toward the low frequency end. The reverse situation is found in electromagnetic (Collins, 1960) or acoustic wave guides (Morse and Ingard, 1968).

For the Cilician Basin, we have estimated the first six cut-off frequencies using $b = 0.17$. The results are given in the table below, where $T_n$ refers to the corresponding periods for the latitude of the Cilician Basin.

| $n$ | 1 | 2 | 3 | 4 | 5 | 6 |
|---|---|---|---|---|---|---|
| $\omega_n \times 10^4$ | 541 | 271 | 180 | 135 | 108 | 90 |
| $T_n$ (days) | 15.7 | 31.4 | 47.1 | 62 | 78.5 | 94 |

*b. Shelf regions*

In the absence of wind-stress the motions in the shelf regions are forced by the interior motion [cf. (2.7) and (2.9)]. When the shelf–interior coupling is ignored the wind-free motions correspond to the continental shelf waves (Buchwald and Adams, 1968; Gill and Schumann, 1974). The corresponding phase velocities for the shelf waves are given by

$$C_n^{(j)} = (-1)^j c_n^{(j)}, \quad (3.6)$$

where

$$c_n^{(j)} = \delta_j/\delta_B(\beta_n^2 + 1/4\delta_B^2), \quad (3.7a)$$

$$\beta_n \cos\beta_n + (1/2\delta_B)\sin\beta_n = 0, \quad (3.7b)$$

with $j = 1, 2$ referring to the shelves along $x = 0$ and $x = 1$ respectively. It is seen from (3.6) that the phase propagation for the shelf along $x = 0$ and for the interior have the same direction, since the depth increases from $x = 0$ to $x = 1$. Beyond $x = 1 - \delta_2$, the depth decreases, leading to a phase propagation direction opposite to that of the interior.

When the forcing by the interior is taken into account, the shelf motions are profoundly altered. To examine the important features of the coupling it is sufficient to consider the $m$th progressive mode of the interior. The forcing in (2.7c) or (2.9c) is then proportional to $\exp ik_m^{\pm}y$. Assuming solutions of the form

$$\Psi^{(1)} = \exp(\xi/2\delta_B) \sum_n \alpha_n^{(1)} \sin\beta_n\xi \exp i(k_m^{\pm}y + \omega t), \quad (3.8a)$$

$$\Psi^{(2)} = \exp(\mu/2\delta_B) \sum_n \alpha_n^{(2)} \sin\beta_n\mu \exp i(k_m^{\pm}y + \omega t), \quad (3.8b)$$

it is a straightforward task to show through (2.7) and (2.9) that

$$\alpha_n^{(1)} \approx 1/\{\kappa_n^{(1)} - k_m^{\pm}\}, \quad (3.9a)$$

$$\alpha_n^{(2)} \approx 1/\{\kappa_n^{(2)} + k_m^{\pm}\}, \quad (3.9b)$$

where

$$\kappa_n^{(j)} \equiv \omega/c_n^{(j)} > 0. \quad (3.10)$$

It follows from (3.9a) that the motions within the shelf along $x = 0$ can be tuned to resonance when $\kappa_n = k_m^{\pm}$. This condition corresponds to the matching of the phase velocity of the $m$th interior mode to that of the $n$th continental shelf wave mode, when the latter is decoupled from the former. No such situation exists (cf. 3.9b) for the shelf along $x = 1$ because the phase propagation directions for the shelf and the interior oppose.

Utilizing (3.3) and (3.10), it is easy to show that the conditions $\kappa_n = k_m^{\pm}$ imply a set of natural frequencies for the motions of the shelf when it is coupled to the interior:

$$\omega_{mn}^2 = \tilde{\omega}_n^2[2 - (\tilde{\omega}_n/\omega_m)^2], \quad (3.11)$$

where $\omega_m$ is given by (3.4), while $\tilde{\omega}_n^2 \equiv bc_n^{(1)}$. Clearly the natural frequencies specified by (3.11) can exist provided $\tilde{\omega}_n/\omega_m < 2^{1/2}$. For fixed $m$, there thus exists a finite number of shelf modes satisfying this condition.

The resonant coupling discussed above is very unlikely to occur for the Cilician Basin. This is because the interior slopes down towards Turkey, the shelf area along northern Cyprus being very steep and narrow ($\delta_1 \to 0$). The shelf waters along the Turkish coast cannot exhibit a resonant tuning at $\omega_{mn}$. However, large amplitude motions can still occur on the shelf whenever the interior itself resonates. In what follows the attention is thus fixed on the interior.

## 4. Forced motions

In all the boundary value problems considered below, we seek solutions of the form

$$\psi = \sum_{n=1}^{\infty} \psi_n(x)\Phi_n(y), \tag{4.1}$$

whence $[\psi_n(x)]$ defined through (3.2) form an orthogonal set such that

$$\int_0^1 H^{-1}\psi_n\psi_m dx = \delta_{mn}/2, \tag{4.2}$$

where $\delta_{mn}$ is the kronecker delta. The solution (4.1) satisfies the boundary condition (2.5). Upon substituting (4.1) into (2.12) and utilizing (4.2), we obtain

$$\Phi_{n,yy} + (2b/i\omega)\Phi_{n,y} - (b/\omega_n)^2\Phi_n = Q_n(y), \tag{4.3}$$

where

$$Q_n = 2\int_0^1 H^{-1}Q\psi_n dx. \tag{4.4}$$

### a. *Infinitely long channel*

We assume that the wind-stress acts within a belt of length $l$ (Fig. 2). In addition, we take $T^x = 0$ and $T^y$ uniform so that $Q = 2bT^y/i\omega$. Other forms of forcing do not alter the substance of the results obtained. Within the wind belt, the general solution of (4.3) is then

$$\Phi_n = -[(b/\omega_n)^2]^{-1}Q_n + A_n \exp(ik_n^+ y) + B_n \exp(ik_n^- y), \quad 0 < y < l, \tag{4.5}$$

where $A_n$, $B_n$ are constants to be determined. Outside the wind belt, $Q_n = 0$ so that the general solution is of the form given in (3.1). To the right of the wind belt ($y < 0$) only $k_n^-$ modes are admissable. This is because in $y < 0$, $k_n^-$ modes imply decaying solutions for $\omega > \omega_n$ and for $\omega < \omega_n$ they yield forward waves radiating to $y \to -\infty$. On similar grounds only the $k_n^+$ modes can be admitted for $y > l$. Consequently

$$\Phi_n = \begin{cases} C_n \exp(ik_n^- y), & y < 0, \\ D_n \exp(ik_n^+ y), & y > l, \end{cases} \tag{4.6}$$

where $C_n$, $D_n$ are constants. The constants in (4.5) and (4.6) are determined by matching the solutions on $y = 0$, $l$ by requiring the continuity of pressure and of the longitudinal velocity. This in turn implies that

$$\Phi_n|_-^+ = 0, \quad \Phi_{n,y}|_-^+ = 0, \tag{4.7}$$

where $|$ implies the differences of values on $y = 0$, $l$. Upon invoking (4.7) there follows

$$\Phi_n = -4bn\pi[1 - (-1)^n e^{-b}]T^y\Phi_n(y)/i\omega, \tag{4.8}$$

where

$$\Phi_n = \begin{cases} 1 + (1/\Delta k_n)[k_n^- \exp(ik_n^+ y) - k_n^+ \exp ik_n^-(y - l)], & 0 \leqslant y \leqslant l, \\ (k_n^-/\Delta k_n)[1 - \exp(-ik_n^+ l)] \exp(ik_n^+ y), & y \geqslant l, \\ (k_n^+/\Delta k_n)\{1 - \exp(-ik_n^- l)\} \exp(ik_n^- y), & y \leqslant 0, \end{cases} \tag{4.9}$$

$$\Delta k_n = k_n^+ - k_n^- = (2b/\omega)[1 - (\omega/\omega_n)^2]^{1/2}, \tag{4.10}$$

and where use has been made of

$$Q_n = 4bn\pi[1 - (-1)^n e^{-b}](\omega_n/b)^2 T^y/i\omega, \tag{4.11}$$

which follows from (4.4) with $T^x = 0$ and $T^y$ = constant.

The solution above implies that an unbounded resonance will occur if $\omega \to \omega_m$ for some $n = m$ for then $\Delta k_m \to 0$. The situation reflects the matching of one of the cutoff frequencies to the frequency of the forcing, in which case energy radiation is prohibited. A bounded resonant response may be achieved at $\omega = \omega_m$ for special lengths $l$ of the wind belt given by $bl/\omega_m = 2s\pi$, where $s$ is a positive integer. A straightforward calculation shows that for such values of $l$ the average work done by the wind stress over one wave-period also vanishes as a result of the special modal structure of the motion. It is also worth noting through (4.8) that, for sufficiently small values of $b$, odd modes $n = 1, 3, 5 \cdots$ are expected to show a more pronounced resonant response. This reflects the modal structure in that the rate of working by a wind system acting uniformly across the channel is not efficient for the even modes. A simple calculation of the integral of $v\tau^y$ across the channel for $x$-independent $\tau^{(y)}$ shows that this is indeed the case.

### b. *Semi-infinite channel*

For this geometry the channel is closed at one end ($y = 0$), with the fluid occupying $y > 0$. The wind-

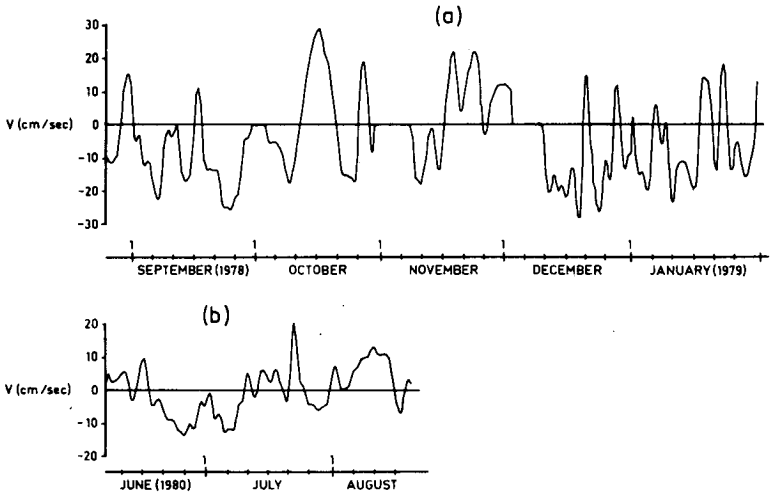


FIG. 5. Time series of longshore velocity during (a) August 1978–January 1979 and (b) June–August 1980.

stress is assumed to act along $y$ and in $0 < y < l$ (Fig. 2). The solution within the wind belt is of the form given by (4.5), while only the $k_n^+$ modes are possible for $y > l$ so that the solution is provided by the second expression in (4.6). The solutions are matched in $y = l$ by making use of (4.7). On $y = 0$ the normal velocity should vanish, implying

$$\Phi_n = 0, \quad y = 0. \tag{4.12}$$

The solution is of the form given in (4.8) with

$$\phi_n = \begin{cases} 1 - \exp(ik_n^+ y) + (k_n^+/\Delta k_n)\exp(-ik_n^- l) \\ \qquad \times [\exp(ik_n^+ y) - \exp(ik_n^- y)], \quad y < l \\ [1 - \exp(ik_n^+ l) + (k_n/\Delta k_n^+)(e^{i\Delta k_n l} - 1)] \\ \qquad \times \exp[ik_n^+(y - l)], \quad y > l. \end{cases} \tag{4.13}$$

The striking feature implied by the above solution is that an unbounded resonance does not occur as $\omega \to \omega_m(\Delta k_m \to 0)$. A numerical summation of the series for representative values of $(x, y, l)$ showed well-pronounced maxima at $\omega = \omega_m$. Therefore, though bounded, a large response does exist at the cutoff frequencies. Since the corresponding energy radiation is zero when $\omega = \omega_m$, a bounded response can only be possible if the average work done by the wind stress over one period and over the entire wind belt vanishes. Again, a straightforward calculation shows this to be the case.

The reason for the bounded response is due to the ways in which the topographic waves reflect from the wall situated at $y = 0$. Specifically, consider the reflection of a progressive mode from the wall. The incident wave from $y > 0$ can only be a $k_n^-$ mode because its energy flux is in the $(-y)$ direction. Upon reflection, this mode must transform into a $k_n^+$ mode, i.e. to a shorter wave because of its radiation property. Upon taking the incident wave amplitude as unity, and invoking the zero flux condition at the wall, we get

$$\Phi_n = \exp(ik_n^- y) - \exp(ik_n^+ y), \tag{4.14}$$

as the $y$ – dependent modal function describing the reflection of an incident wave. Utilizing the expressions

$$V_n = -\psi_{n,x}\Phi_n/H, \quad U_n = \psi_n\Phi_{n,y}/H, \tag{4.15}$$

together with (4.14), it is seen that upon reflection positive particle displacements with longer wavelengths become negative displacements with shorter wavelengths. As $\omega \to \omega_n$ a total cancellation will occur resulting in zero motion everywhere. A similar situation exists in a semi-infinite membrane clamped along $y = 0$ and $x = 0, 1$. As a result of the 180° phase-shift encountered in reflection, a resonant tuning by the forced agency can only lead to a partial success.

The analysis of the forced motion for the case in which the fluid occupies $y < 0$ with a wind belt in $-l < y < 0$ proceeds on the same lines. However, the radiated wave is now a $k_n^-$ mode.

### c. *Rectangular basin*

Consider a rectangular basin formed by placing two walls on $y = 0$ and $y = l$. The boundary conditions on the walls are given by

$$\Phi_n = 0, \quad y = 0, l. \tag{4.16}$$

For an arbitrary distribution of $Q_n(y)$ in (4.3) we seek solutions of (4.3) of the form

$$\Phi_n = \exp(iby/\omega) \sum_{m=1}^{\infty} a_{mn} \sin(m\pi y/l) \tag{4.17}$$

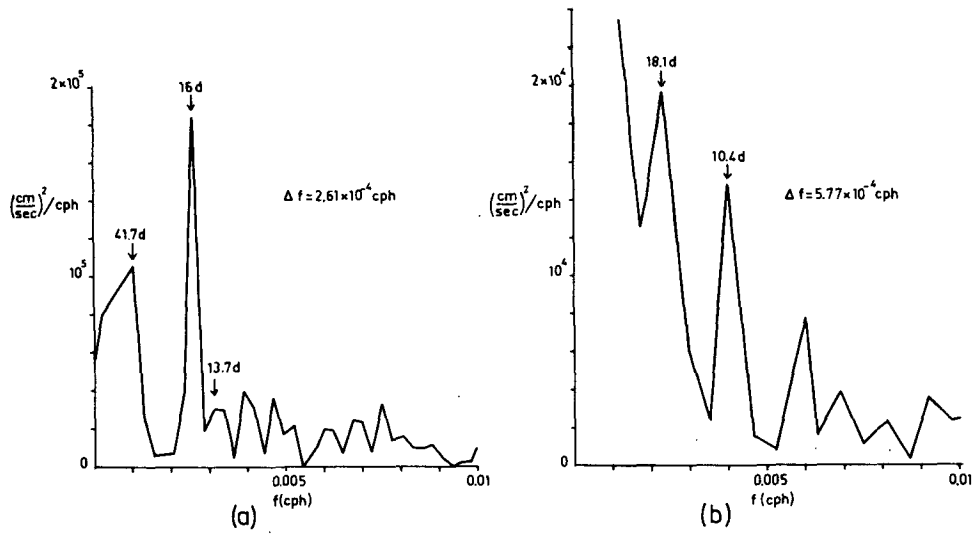


FIG. 6. Energy spectrum of longshore velocity for (a) the period August 1978—January 1979 and (b) June—August 1980.

which satisfies (4.16). Upon substituting (4.17) into (4.3) and utilizing the orthogonality of $(\sin m\pi y/l)$ it is found that

$$a_{mn} = 2\int_0^l Q_n(y)\exp(iby/\omega)\sin(m\pi y/l)/ [(b/\omega)^2 - (b/\omega_n)^2 - (m\pi/l)^2]dy. \quad (4.18)$$

Accordingly, a resonant response will occur when $\omega = \omega_{mn}$, where

$$\omega_{mn} = \omega_n\{1 + (m\pi\omega_n/bl)^2\}^{-1/2} \approx \omega_n\{1 + (m/nl)^2\}^{-1/2}, \quad (4.19)$$

the approximate result being valid when $b \ll 1$. For $l \gg 1$, $\omega_{mn} \approx \omega_n$ for the lowest modes. For the Cilician basin, $l \approx 3$, so that for the lowest modes the resonant frequencies should be approximated well by $\omega_n$. Note that, in general, the closely-packed spectral lines are made denser by the introduction of the walls. It should also be noted that for the closed basin resonance can never occur exactly at $\omega_n$.

## 5. Observations and comparison

Long-term current data encompassing the periods 26 August 1978–31 January 1979 and 6 June–18 August 1980 were collected 3 km off Erdemli in 35 m of water (Fig. 1). Only a single current meter (Aanderaa RCM4) was deployed. A taut-mooring system was utilized with the current meter 20 m below the surface. The instrument was serviced monthly. In essence, the first of these simple observational experiments was carried out as a prelude to the assessment of the variability in time of the local current systems. The second experiment of shorter duration was made for a different study. Simultaneous measurements of wind velocity and of sea level were made but will be reported separately, together with other current measurements taken west of the site. It is sufficient here to consider the currents alone.

The current meter was set to record at 10 min intervals. The digital current records were decomposed into alongshore (NE 45°) and onshore components. The data were then low-passed by taking 30 h moving averages. The onshore low-frequency motions are found to be negligible (below 5 cm $s^{-1}$). Most of the kinetic energy is in the low-passed alongshore component ($v$) whose time histories for the two different measurement periods are given in Fig. 5. The energy spectra of $v$ are given in Fig. 6.

Consider first the spectrum of the longshore current for the longer period (~5 months) measurements. The spectrum contains a sharp primary peak at 16 day = 0.0026 cph (Fig. 6a). A broader secondary peak is located at 41.7 day = 0.001 cph. Smaller peaks located around 13.7 days, 10.4 days, etc., are also present.

From a theoretical point of view, the shelf motions should intensify at the cutoff frequencies of the interior because they are driven by the interior. In other words, resonant response off the shelf break should be detectable on the shelf. Acting on this premise, it is seen that the estimated first cutoff frequency (see table in Section 3) at 15.7 days coincides with the location of the primary peak at 16 days in Fig. 6a. The period of 41.7 days of the second peak in the spectra is close to the third cutoff frequency of 47.1 days. The absence of a spectral peak at the second cutoff frequency estimated as 31.4 days is as expected. This is because a weak response at the even

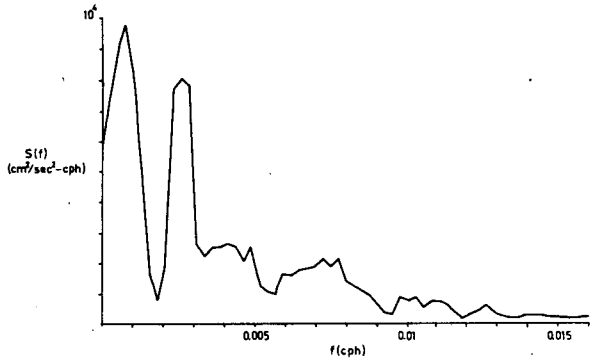


FIG. 7. Sample spectrum with three-point (Deniell) smoothing. 80% confidence limits for the true spectrum: $0.6S(f)$–$2.2S(f)$.

modes is anticipated whenever the wind stress is sufficiently uniform.

The data length is insufficient to discuss the higher modes anticipated at the low-frequency end. The particular ordering of the cutoff frequencies toward the low-frequency end brings about the unfortunate requirement of a very long data base. In fact, it is evident that the 5-month data base is not even sufficient for placing reasonable confidence limits on the spectral estimates. Nevertheless, we did carry out a three-point smoothing of the spectrum shown in Fig. 6a. The result is shown in Fig. 7. The 16-day band corresponding to the first resonant mode clearly survives.

On testing of the theoretical predictions concerned with the first resonant mode, more confidence can be gained by the consideration of the measurements taken during a different period. It is seen in Fig. 6b that a significant number of fluctuations around the 16-day band were present during June–August, 1980. The differences in the magnitudes of the spectral estimates in Figs. 6a and 6b correspond to a factor of $\sim 2$ in the amplitude of oscillations for the two different periods. This can also be inferred from the time series shown in Fig. 5.

An interesting question can be raised with regard to the long-period astronomical effects that may be present within and near the 16-day band. Specifically, one should consider the lunar fortnightly (13.66 days) oscillations and those due to the nonlinear interaction of the $M_2$, $S_2$ tides (14.68 days). The resolution ($\sim 2.6 \times 10^{-4}$ cph) of the raw spectral estimate in Fig. 6a should be sufficiently small for the detection of the lunar fortnightly oscillations but not for $M_2S_2$ tide. Indeed, a small peak is located near a period of 13.7 days. It is, however, very unlikely that the long-period tides alone can be significant. The tides of the region are notoriously small ($\sim 35$ cm) and the fortnightly oscillations yet smaller. It is felt that the nonlinear interaction of such small oscillations should also be negligible. Whether such oscillations can act as external forces as in the sense of winds to generate, indirectly, a resonant response of the basin in the 16-day band is difficult to answer at this stage.

Finally, the spectral peaks above 0.0637 cpd cannot be explained in terms of topographic Rossby waves of the interior. These appear to be related to internal Kelvin and shelf waves. Work on this is in progress and will be reported shortly. In any event, their relatively smaller amplitudes are indicative of the importance of the coupling to the interior.

## 6. Summary and conclusions

A channel flanked by shelf areas forms a system of coupled wave guides. When the shelf areas are narrow and steep the interior is decoupled from the motions in the shelf regions and provides partial forcing. The topographic Rossby waves and a set of evanescent motions form the basic modes of the interior. The shelf for which the bottom slope has the same sign as that of the channel proper can be tuned into resonance by the interior. Such a tuning is not possible for the Cilician Basin. However, the interior itself can resonate at the cutoff frequencies and transmit this response to the shelf areas. This should especially be the case when the shelf is narrow and its waters deep (as it is in the present study area) for then the frictional attenuation is expected to be small.

The present results indicate that the low-frequency motions on the southeastern shelf waters of Turkey are intimately related to what happens off the shelf. A continental-shelf wave study that neglects the coupling to the deep waters and considers only the locally wind-driven shelf waves is not appropriate for the northeastern coastal margins of the Cilician Basin. The situation is reminiscent of Garvine's (1971) results, where it was found that the offshore pressure gradients play a crucial role in steady-state coastal upwelling.

Several requirements are placed on the observational experiments because the cutoff frequencies and the spacings between them diminish rapidly with increasing mode number. The intervals between them decrease as $fb/\pi n^2$. For $b \simeq 0.17$ this implies that the resolution of the 5th and 6th cutoff frequencies will require nearly a year of measurements. Nevertheless, the partial support found from five months of observations leaves much to be desired. A set of experiments much expanded in scope and duration is underway and will be reported later.

*Acknowledgment.* This work was partially supported by UNEP/IOC, MED VI Pilot project. The question of the astronomical tides was raised by one of the referees. Dr. E. Özsoy helped considerably with data processing.

## REFERENCES


Adams, J. K., and V. T. Buchwald, 1969: The generation of continental shelf waves. *J. Fluid Mech.*, **35**, 815–826.

Allen, J. S., 1976: On forced, long continental-shelf waves on an *f*-plane. *J. Phys. Oceanogr.*, **6**, 426–431.

Brooks, D. A., and C. N. K. Mooers, 1977: Free, stable continental-shelf waves in sheared, barotropic boundary currents. *J. Phys. Oceanogr.*, **7**, 380–388.

Buchwald, V. T., and J. K. Adams, 1968: The propagation of continental shelf waves. *Proc. Roy. Soc. London*, **A305**, 235–250.

Bunker, A. F., and M. C. Cornell, 1971: Wintertime interactions of the atmosphere with the Mediterranean Sea. Woods Hole Oceanographic Institution, Ref. No. 71-61, 36 pp.

Collin, R. E., 1960: *Field Theory of Guided Waves*. McGraw-Hill, 606 pp.

Fofonoff, N. P., 1962: Dynamics of ocean currents. *The Sea*, Vol. 1, M. N. Hill, Ed., Interscience, 323–395.

Garvine, R. W., 1971: A simple model of coastal upwelling dynamics. *J. Phys. Oceanogr.*, **1**, 169–170.

Gill, A. E., and E. H. Schumann, 1974: The generation of long shelf waves by wind. *J. Phys. Oceanogr.*, **4**, 83–90.

Hydrographer of the Navy (U.K.), 1976: *Mediterranean Pilot*, Vol. 6, 171 pp.

Lacombe, H., and P. Tchernia, 1972: Caracteres Hydrologiques et circulation des eaux en Mediterranee. *The Mediterranean Sea*, Dowden, Hutchinson and Ross, 25–36.

LeBlond, P. H., and L. A. Mysak, 1978: *Waves in the Ocean*. Elsevier, 602 pp.

Morse, P. M., and K. U. Ingard, 1968: *Theoretical Acoustics*. McGraw-Hill, 927 pp.

Palmén, E., and C. W. Newton, 1969: *Atmospheric Circulation Systems*. Academic Press, 603 pp.

Pedlosky, J., 1979: *Geophysical Fluid Dynamics*. Springer-Verlag, 624 pp.

Royal Netherlands Meteorological Institute, 1957: *The Mediterranean*. 91 pp.

Tibaldi, S., 1979: Lee cyclogenesis and its numerical simulation, with special attention to the Alpine region: A review. *Geophys. Astrophys. Fluid Dyn.*, **13**, 25–49.